Published in final edited form as:
J Cell Physiol. 2012 July ; 227(7): 2907–2916. doi:10.1002/jcp.23035.

Engineered Endothelial Progenitor Cells That Overexpress Prostacyclin Protect Vascular Cells

Qi Liu[1], **Yutao Xi**[1,‡], **Toya Terry**[1,‡], **Shui-Ping So**[2], **Anita Mohite**[2], **Jia Zhang**[1], **Geru Wu**[1], **Xiaobing Liu**[1], **Jie Cheng**[1], **Ke-He Ruan**[2], **James T. Willerson**[1], and **Richard A.F. Dixon**[1,*]

[1]The Texas Heart Institute at St. Luke's Episcopal Hospital, Houston, TX 77030

[2]The University of Houston College of Pharmacy, Houston, TX 77004

Abstract

Prostacyclin (PGI2) is a potent vasodilator and important mediator of vascular homeostasis; however, its clinical use is limited because of its short (<2 minute) half-life. Thus, we hypothesize that the use of engineered endothelial progenitor cells (EPCs) that constitutively secrete high levels of PGI2 may overcome this limitation of PGI2 therapy. A cDNA encoding COX-1-10aa-PGIS, which links human cyclooxygenase-1(COX-1) to prostacyclin synthase (PGIS), was delivered via nucleofection into outgrowth endothelial progenitor cells (EPCs) derived from rat bone marrow mononuclear cells. PGI2-secreting strains (PGI2-EPCs) were established by continuous subculturing of transfected cells under G418 selection. Genomic PCR, RT-PCR, and Western blot analyses confirmed the overexpression of COX-1-10aa-PGIS in PGI2-EPCs. PGI2-EPCs secreted significantly higher levels of PGI2 in vitro than native EPCs (P<0.05) and showed higher intrinsic angiogenic capability; conditioned medium from PGI2-EPCs promoted better tube formation than conditioned medium from native EPCs (P<0.05). Cell- and paracrine-mediated in vitro angiogenesis was attenuated when COX-1-10aa-PGIS protein expression was knocked down. Whole-cell patch-clamp studies showed that 4-aminopyridine–sensitive K^+ current density was increased significantly in rat smooth muscle cells (rSMCs) cocultured under hypoxia with PGI2-EPCs (7.50±1.59pA/pF, P<0.05.) compared with rSMCs cocultured with native EPCs (3.99±1.26 pA/pF.). In conclusion, we successfully created EPC strains that overexpress an active novel enzyme resulting in consistent secretion of PGI2. PGI2-EPCs showed enhanced intrinsic proangiogenic properties and provided favorable paracrine-mediated cellular protections, including promoting in-vitro angiogenesis of native EPCs and hyperpolarization of SMCs under hypoxia.

Keywords

endothelial progenitor cells; prostacyclin; angiogenesis; paracrine; patch clamp

Introduction

Prostacyclin (PGI2) is synthesized in endothelial cells from arachadonic acid in a multistep process involving the coupling of cyclooxygenase (COX) isoenzymes COX-1 or COX-2 to prostacyclin synthase (PGIS) (Mitchell and Warner, 2006; Moncada et al., 1976). PGI2

*Address for correspondence: Richard A.F. Dixon, Texas Heart Institute, MC2-255, Houston, TX 77030, USA, Tel: 832-355-9137, Fax: 832-355-9333. rdixon@heart.thi.tmc.edu.
‡These authors contributed equally to this work

Conflicts of Interest
None

provides vasoprotection through its vasodilative, anti-inflammatory, and antithrombotic properties (Liu et al., 2005; Murata et al., 1997). Because of these beneficial effects, PGI2 has been used to treat diseases characterized by endothelial dysfunction such as pulmonary arterial hypertension (PAH) (Badesch et al., 2004). Despite the promising clinical benefits, PGI2 therapy is cumbersome. Patients have to use a continuous-infusion pump to administer PGI2 exogenously because of its short circulating half-life of 1 to 2 minutes (Barst et al., 1996). Longer-acting analogues are available but are thought to be less efficacious than PGI2. To maintain the potency and circumvent the instability of PGI2, a strategy must be developed to promote the constant in vivo biosynthesis of PGI2 from a biologically relevant cellular source. This approach would be vastly superior to the current exogenous pharmaceutical route.

Because endothelial cells have limited proliferative and regenerative ability, endothelial progenitor cells (EPCs) have emerged as a promising resource for neovascularization (Asahara et al., 1997; Shi et al., 1998). Accumulating evidence indicates that bone marrow–derived EPCs mobilize to the site of vascular damage and participate in re-endothelialization and vascular repair (Asahara et al., 1999; Takahashi et al., 1999). Endogenous secretion of PGI2 by EPCs facilitates vascular regeneration (He et al., 2008; Numaguchi et al., 1999). However, impaired function of EPCs is associated with decreased endogenous PGI2synthesis or signaling (Kawabe et al., 2010). The potency of EPCs under pathologic conditions may be improved by developing ways to enhance their intrinsic PGI2 production.

In the present study, using the nonviral transfection technique of nucleofection, we produced 2 strains of rat bone marrow–derived outgrowth EPCs that constitutively overproduce PGI2(PGI2-EPCs) by introducing an active triple-catalytic enzyme that links cyclooxygenase-1 to prostacyclin synthase (COX-1-10aa-PGIS). This triple-catalytic enzyme catalyzes 3 key reactions that allow the production of PGI2 from arachidonic acid (AA) (Ruan et al., 2008). We have shown that PGI2-EPCs secrete higher levels of PGI2 and have better intrinisic angiogenic abilities than native EPCs. Furthermore, PGI2-EPCs showed beneficial paracrine effects on angiogenesis in native EPCs and on vascular smooth muscle cell (SMC) hyperpolarization. These functions are crucial for new blood vessel formation and regulation of vascular homeostasis.

Materials and Methods

Stable transfection of outgrowth EPCs with a plasmid expressing a novel triple-catalytic hybrid enzyme

All animal experiments were conducted in accordance with the guidelines of the University of Texas Health Science Center Animal Welfare Committee. Fisher-344 rats (8–12 weeks old; n=5; Charles River Laboratories, Wilmington, MA) were humanely euthanized, and the femurs and tibiae were flushed with cold Dulbecco's phosphate-buffered saline (DPBS, Invitrogen, Carlsbad, CA). The aspirated bone marrow cell suspension was filtered with 40-μm cell strainers and was centrifuged at 1100 rpm for 5 minutes. Bone marrow cells were resuspended and centrifuged on a Ficoll gradient (Ficoll-Paque Plus, GE Healthcare, Piscataway, NJ) to isolate bone marrow mononuclear cells (MNCs), which were then washed 2 times with DPBS. To culture MNCs, we followed the procedures described by Ingram et al (Ingram et al., 2004), with minor modification. Briefly, MNCs were seeded onto 6-well collagen-I coated plates (BD Falcon) in endothelial cell growth medium-2 (EBM-2, Lonza, Switzerland) supplemented with human fibroblast growth factor-2, vascular endothelial growth factor (VEGF), R3-insulin-like growth factor-1, human epidermal growth factor, hydrocortisone, ascorbic acid, GA-1000,heparin(Lonza), and 10% fetal bovine serum (Invitrogen). The plates were placed into a 5% CO_2 incubator at 37°C. After 24 hours of culture, non-adherent cells were aspirated, and fresh culture medium was added

to continue culture of adherent cells. The medium was changed daily during the first 2 weeks of culture. After 7 days of culture, outgrowing cell clusters consisting of cobblestone-shaped cells appeared. Confluent cell monolayers were dissociated by using StemPro Accutase (Invitrogen) and passaged onto collagen-I coated tissue culture dishes (60 or 100 mm, BD Falcon). At passages 3–4, cells were characterized by flow cytometry analysis and in vitro angiogenesis assays as described below.

Cells with EPC properties were transfected by using the Amaxa Nucleofector System (Basic Endothelial Cell Nucleofector Kit, Lonza) to introduce a plasmid expressing a novel triple-catalytic hybrid enzyme that links COX-1 to PGIS (COX-1-10aa-PGIS). The plasmid (pcDNA3.1, Invitrogen) contains human cytomegalovirus promoter and neomycin resistance gene for selection of stable cell lines (Ruan et al., 2008). After nucleofection, cells were grown under G418 (Invitrogen) selection for 2 to 3 weeks. Then, cell clusters were selected for subculture under endothelial conditions (described above) supplemented with G418. Passages were counted once cells were expanded. Confluent cell monolayers at passages 10 to 21 were harvested for evaluation of stable expression of the transgene COX-1-10aa-PGIS. EPCs that overexpress COX-1-10aa-PGIS are referred to as PGI2-EPCs.

Flow cytometry

Outgrowth EPCs (native EPCs) and PGI2-EPCs were detached from the culture plates by using StemPro Accutase, washed, and suspended at 1×10^6 cells per tube in 500 μl of cold DPBS. Cells were then incubated with polyclonal goat anti-rat CD14 (Santa Cruz Biotechnology; T-19) or FITC-conjugated anti-rat CD45 (Invitrogen) for 30 min at 4°C. For indirect staining, cells were rinsed in DPBS and then incubated with the FITC-conjugated donkey anti-goat IgG (Abcam) for an additional 30 min at 4°C. Permeabilization steps were used prior to the following antibody staining; briefly, cells were incubated with a 2% paraformaldehyde solution for 10 minutes at room temperature (RT). Cells were washed, centrifuged, and resuspended in 1X Perm/Wash Buffer I (BD Bioscience) for 15 minutes at RT in the dark. Cells were washed and suspended at 1×10^6 cells per tube in 500 μl of buffer. Subsequently, cells were incubated with polyclonal goat anti-rat CD31, or anti-rat CD34 (R&D Systems) antibody for 30 min at 4°C, followed by incubation with the FITC-conjugated donkey anti-goat IgG (Abcam) antibody for 30 min at 4°C. In addition, permeabilized cell staining included incubation with polyclonal rabbit anti-rat VEFGR-2 (Abcam) or vWF (Abcam) antibody for 30 min at 4°C, followed by incubation with the FITC-conjugated goat anti-rabbit IgG (Abcam) antibody for 30 min at 4°C. Fluorochrome- and isotype-matched controls were used in parallel experiments to monitor nonspecific staining. All data were recorded with a BD FACS LSRII and analyzed with FlowJo 7.6.1.

Genomic PCR, RT-PCR, and Western blot

Genomic DNA was isolated and purified from PGI2-EPCs and native EPCs according to the manufacturer's protocol (DNeasy Blood and Tissue Kit, QIAGEN, Germantown, MD). The purity and concentration of isolated DNA were estimated by using an Eppendorf BioPhotometer plus 6132 instrument. PCR was carried out using total DNA (200ng), COX-1-10aa-PGIS specific primers, and platinum Taq DNA polymerase (Invitrogen). The size of the PCR product (445 bp spanning the 10aa linker region of COX-1-10aa-PGIS) was determined by comparison to a 100bp DNA ladder under UV light after running 2% agarose gel electrophoresis.

RNA was isolated from PGI2-EPCs and native EPCs according to the manufacturer's protocol (RNeasy Plus Micro Kit, QIAGEN). The purity of RNA was estimated by the A_{260}/A_{280} ratio (NanoDrop 1000 Spectrophotometer, Thermo Scientific, Waltham, MA). Total RNA (200ng) was reverse transcribed by using the oligo dT primer and superscript III first

strand synthesis system (Invitrogen). PCR was subsequently carried out with human COX-1 and PGIS-specific primer pairs and platinum Taq DNA polymerase (Invitrogen). The primers were designed by using Primer-Blast provided by NCBI. The size of PCR products was determined by comparison to a 100bp DNA ladder (Invitrogen) under UV light after 1–2% agarose gel electrophoresis.

Membrane fractions of the cell lysates prepared from native EPCs and PGI2-EPCs were used to assess the expression of the novel fusion protein (COX-1-10aa-PGIS, 130kD) by Western blot. In brief, 5 μg of protein was fractionated by SDS-PAGE (4%–20% gradient gel, Bio-Rad, Hercules, CA) and transferred onto a PVDF membrane. The membrane was probed with a primary antibody against human PGIS (No 160640,Cayman Chemical, Ann Arbor, MI) followed by an HRP-conjugated anti-rabbit secondary antibody (Sigma, St. Louis, MO). Protein signals were detected by using the ECL system (Thermo Scientific). To verify equal loading of each protein sample, membranes were stripped and reprobed with the membrane marker Na^+/K^+ ATPase monoclonal antibody (Abcam). Western blot assay was also used to examine rat endogenous COX-1 and COX-2 expression in native EPCs and PGI2-EPCs. Briefly, the protein was transferred to a PVDF membrane, and a COX-1 (clone CX111, Cayman Chemical) or COX-2 monoclonal antibody (sc-19999, Santa Cruze Biotechnology) was added, followed by a HRP-conjugated anti-mouse secondary antibody (Sigma).

6-keto prostaglandin F1α and thromboxane B2 enzyme immunoassay

The secretion of PGI2 and thromboxane A2 (TXA2) in the supernatant from native EPCs and PGI2-EPC strains was measured by using the 6-keto prostaglandin F1α and thromboxane B2 (TXB2) enzyme immunoassay kits (Cayman Chemical), according to the manufacturer's instructions. The supernatant was collected after incubating cells (5×10^5) with serum-free EGM-2 (containing 0.1% BSA) for 24 hours at 37°C. The absorbance was read using a microplate reader (Safire II, Tecan, Triangle Park, NC), and the concentration (pg/ml) of 6-keto prostaglandin F1α and TXB2 was calculated for each sample by using XFluor4 Safire II, V4.62n software.

Cell proliferation and apoptosis assays

Proliferation of native EPCs and PGI2-EPCs was quantified by using the 5-Bromo-2-deoxy-uridine (BrdU) labeling and detection kit III according to the manufacturer's instructions (Roche Applied Science, Indianapolis, IN). Briefly, cells were seeded on 96-well plates (1×10^4/well) and incubated with EGM-2 growth medium in a 5% CO_2 incubator at 37°C for 24 hours. The medium was switched to EGM-2 containing 10μM BrdU, and cells were incubated for an additional 2 hours. BrdU incorporation into cellular DNA was measured by using a microplate reader (Safire II, Tecan). Three independent experiments were performed, and each assay was carried out in triplicate.

For apoptosis assays, native EPCs and PGI2-EPCs were plated in 96-well plates (1×10^4/well) and cultured in EGM-2 growth medium for 24 hours. Cells were then incubated with serum-free EGM-2 for an additional 24 hours, followed by incubation with 200 nM of hydrogen peroxide (H_2O_2, diluted in serum- free EGM-2 medium) for 4 hours to induce apoptosis. Caspase-3/7 activities were measured by using the Apo-One Homogeneous Caspase-3/7 Assay kit, according to the manufacturer's instructions (Promega).

In vitro angiogenesis

Outgrowth native EPCs (control) and PGI2-EPCs were trypsinized, washed, and collected. A collagen-based reduced growth factor membrane matrix (Geltrex, Invitrogen) was coated (50 μl/cm^2) onto 24-well plates, which were incubated for 30 minutes to allow the gel to

solidify. Then, approximately 3.5×10^4 EPCs were resuspended in 200μl/cm^2 of EGM-2, seeded onto 24-well plates, and placed in an incubator (37°C, 20% O_2, 5% CO_2) to allow for tube formation. Each hour, tube formation was documented until a pronounced difference between control EPCs and PGI2-EPCs was observed. Assays were performed in triplicate. Cell viability was confirmed by Calcein AM staining (Invitrogen). Digital images were taken using an inverted light microscope (Olympus IX71, Leeds Instruments, Irving, TX) at a 40× magnification for all experiments. Images were taken in 3 different fields per condition, and the total cumulative tube length (μm) was measured. NIH Image*J* software was used to analyze the data.

Additionally, the conditioned medium (CM) of native EPCs and PGI2-EPCs was used to examine paracrine-mediated in vitro angiogenesis. Cells were seeded onto 24-well plates (1×10^5 cells/well) with EGM-2 and incubated overnight. EGM-2 was removed, and serum-free EGM-2 was added to the wells, which were incubated at 37°C for an additional 24 hours. Supernatant (CM) from EPC or PGI2-EPC cultures was collected and used in the above described tube formation assays performed in triplicate with native EPCs (control). Images were taken, and the data were analyzed as described above.

Whole-cell patch-clamp studies

Native EPCs or PGI2-EPCs (5×10^4) were cocultured for 12 hours with rat vascular SMCs (rSMCs, Lonza) under normal (20% O_2, 5% CO_2, 37°C) or hypoxic (1.1% O_2, 5% CO_2, 37°C) conditions in a double-chamber transwell culture system (BD Falcon, Rockville, MD). SMCs were harvested, and the single-cell K+ current (I_K) was measured using the whole-cell patch-clamp technique with an Axopatch 200B amplifier and a CV-4 headstage (Axon Instruments Inc., Union City, CA). To record the I_K, we continuously superfused cells with normal Tyrode's solution (mmol/L): 130 NaCl, 4 KCl, 1.8 $CaCl_2$, 1 $MgCl_2$, 24 $NaHCO_3$, 1.2 NaH_2PO_4, and 10 glucose (pH 7.35). The pipette solution to record I_K contained (mmol/L) the following: 120 K-aspartate, 10 Na_2ATP, 2 $MgCl_2$, 10 EGTA, and 10 HEPES (pH 7.35 with KOH). Data were acquired in PCLAMP version 9.0 (Axon Instruments, Sunnyvale, CA). The digitization rate was 5 KHz, and the cut-off frequency for filtration was 2 KHz. In a single cell, current-voltage (I–V) relations for steady-state current were measured at the end of 400-ms pulses to voltages between −50 and +70mV at a constant holding potential −60mV. The currents were expressed in picoamperes per picofarad (pA/pF) to normalize the differences in cell membrane area in single vascular SMCs. All experiments were performed at RT.

Human PGIS and COX-1 knockdown in PGI2-EPCs by small interfering RNA

PGI2-EPCs (2×10^5/well) were seeded onto 6-well tissue-culture plates for 24 hours before transfection with human scrambled siRNA control, human PGIS siRNA or human COX-1 siRNA (1 μM, Santa Cruz Biotechnology, Inc., Santa Cruz, CA). Transfection was conducted according to the manufacturer's protocol (Santa Cruz Biotechnology, Inc.). Fresh EGM-2 medium was added to the cells 8 hours after transfection. At 24 hours after transfection, EGM-2 was replaced with serum-free EGM-2 and the cells were incubated for an additional 72 hours. Supernatant from each transfection condition was collected at 24 hour intervals up to 96 hours. Cells were then replenished with fresh serum-free EGM-2. Supernatant collected at the 72 hour interval was used to measure the 6-keto prostaglandin F1α production, as described above. At the 96 hour interval, the cells and CM were used for western blot and in vitro angiogenesis experiments.

Statistical analysis

Data were expressed as the mean ± standard error of mean (SEM). One-way analysis of variance (ANOVA) with the Mann-Whitney post hoc test and *t*-test were used to determine

the statistical significance within and between groups (GraphPad Prism 5). $P<0.05$ was considered statistically significant.

Results

Phenotypic properties of rat outgrowth EPCs

Using a method for culturing putative human endothelial colony-forming cells (Ingram et al., 2004), we isolated and expanded ex vivo a subtype of primary colony-forming cells from rat bone marrow mononuclear cells. The outgrowing cell colonies emerged after 1 week of culture (Fig. 1A and 1B) and formed a confluent monolayer with a cobblestone-like appearance (Fig. 1C). At early passages (P3–4), immunophenotyping by flow cytometry indicated that this population expresses the endothelial markers, including platelet endothelial cell adhesion molecule-1 (CD31), CD34, Von Willebrand factor (vWF), VEGF receptor-2 (VEGFR-2), but not the hematopoietic cell surface markers CD14 and CD45 (Fig. 1D). Our in vitro angiogenesis assay showed that this cell type formed capillary-like structures when seeded on extracellular matrix–precoated plates (Fig. 1E and 1F). Thus, this cell population displays the properties of outgrowth EPCs.

Identification of PGI2-EPC strains that consistently overexpress triple-catalytic hybrid enzyme COX-1-10aa-PGIS

To engineer outgrowth EPCs that overexpress PGI2, we constructed a plasmid that expresses a novel triple-catalytic hybrid enzyme that links human COX-1 to PGIS (pCOX-1-10aa-PGIS). Using nucleofection, we introduced the pCOX-1-10aa-PGIS plasmid into cells and continuously subcultured the transfected cells under G418 selection. Multiple G418 resistant cell strains were developed and maintained under endothelial cell culture conditions for 1–2 months before identifying transgene expression.

Genomic PCR was used to examine the integration of the COX-1-10aa-PGIS gene into the host cell genome. To ensure recognition of the intact transgene, PCR primers were designed to encompass the 10 amino-acid linker region that connects COX-1 and PGIS. We detected the human COX-1-10aa-PGIS transgene in the host genome of 2 EPC strains (PGI2-EPC strain 1 and 2) (Fig. 2A). The transcript from the human COX-1-10aa-PGIS transgene in both strains was further examined by RT-PCR (Fig. 2B). PCR primers specifically recognized human COX-1or PGIS cDNA, as opposed to endogenous rat cDNA. Furthermore, western blot analysis confirmed the expression of the novel fusion protein (COX-1-10aa-PGIS, 130 kD) in PGI2-EPC strains 1 and 2 (Fig. 2C). Endogenous rat COX-1 and COX-2 protein expression was also examined by Western blot. Both native EPCs and PGI2-EPC strains expressed a comparable level of COX-1(70 kD, Fig. 2C). No endogenous COX-2 (72 kD) was detected in native or PGI2 EPCs (Fig. 2C).

To assess whether PGI2-EPC strains consistently produced significantly higher levels of PGI2 than native EPCs (control), we measured PGI2 secretion at early (P10) and late (P21) cell passages. To examine PGI2 production, we used an enzyme immunoassay to measure the metabolite 6-keto PGF1α in the supernatant of native EPCs and PGI2-EPC because of the short half-life of PGI2. Compared with control cells, the concentration of 6-keto PGF1α was 4.7±0.3-fold higher in strain 1 ($P<0.01$, n=3) and 3.6±0.6-fold higher in strain 2 ($P<0.01$, n=3) cells at the P10 passage (Fig. 2D). The increased release of PGI2 from PGI2-EPC strains was also seen at the P21 passage; PGI2-EPC strains 1 and 2 secreted 4.9±0.9-fold and 3.9±0.6 fold higher levels of 6-keto PGF1α, respectively, compared to native EPCs ($P<0.01$, for both comparisons; n=3). However, both native EPCs and PGI2-EPC strains showed in vitro signs of cellular aging (ie, increased cell size, flattened appearance, and

decreased proliferation) after 25 passages (cells were passaged every 3–4 days). Therefore, we used cells before the 22nd passage for all in vitro assays.

We analyzed endothelial maker expression in PGI2-EPC strains 1 and 2 by immunophenotypic analysis via flow cytometry. We found that PGI2-EPC strains retained a similar level of CD31, CD34, vWF, VEGFR-2, CD14, and CD45 expression as their native counterparts (Fig. 2E). Together, our data clearly show that we have successfully established PGI2-EPC stains that stably express the novel active human COX-1-10aa-PGIS enzyme and that produce higher levels of PGI2 than native EPCs.

Effect of triple-catalytic hybrid enzyme COX-1-10aa-PGIS on cell proliferation and apoptosis

We evaluated the effect of overexpression of COX-1-10aa-PGIS in PGI2-EPC strains 1 and 2 on cell proliferation by comparing BrdU incorporation into replicating DNA in PGI2-EPCs and native EPCs. No significant difference was detected between groups (Fig. 3A, $P>0.05$, n=3), suggesting PGI2-EPCs and native EPCs propagate at a similar rate. We also examined the anti-apoptotic effect of PGI2-EPC strains by measuring the activity of caspase-3/7 after induction of apoptosis by H_2O_2 (200 nM). Both PGI2-EPC strains showed significantly less caspase-3/7 activity than native EPCs (EPC vs strain 1, $P<0.01$, n=3; EPC vs strain 2, $P<0.01$, n=3), indicating the enhanced protective property of PGI2-EPCs (Fig. 3B).

Because counteracting the effect of TXA2 is a primary physiologic function of PGI2, we examined TXA2 production in PGI2-EPC strains. We used an enzyme immunoassay to measure TXB2 (the metabolite of TXA2) in the supernatant of native EPCs and PGI2-EPC strains because of the unstable nature of TXA2. Our results suggested that PGI2-EPC strains and native EPCs secrete a similar amount of TXA2 (Fig. 3C).

PGI2-EPCs show enhanced angiogenic properties

To assess the angiogenic ability of native EPCs (control) and PGI2-EPC strains, we evaluated their capacity to form capillary-like networks in vitro. Cells were seeded on a reduced growth factor–membrane matrix and incubated until a pronounced difference was observed between control and PGI2-EPCs. As early as 4 hours after seeding, the total tube length of both PGI2-EPC strains was significantly increased compared with control EPCs (Fig. 4A and 4B; $P<0.05$; n=3). To assess whether PGI2-EPCs promote paracrine-related angiogenesis, we collected CM from PGI2-EPCs and control EPCs, respectively, and mixed native EPCs with each individual CM. CM from PGI2-EPC strains markedly stimulated endothelial tube formation in native EPCs. The total length of tubes of native EPCs incubated with strain 1 or strain 2 CM was significantly increased compared to tube length of native EPCs incubated with control CM (Fig. 4C, 4D; $P<0.05$; n=3).

To determine if the enhanced angiogenesis of PGI2-EPCs was induced by the expression of the hybrid enzyme (COX-1-10aa-PGIS), we knocked down hybrid enzyme expression in PGI2-EPC strain 1 by using pools of human specific siRNA to target the different sequence region within PGIS mRNA. This approach resulted in significant knockdown of expression of the human COX-1-10aa-PGIS protein in PGI2-EPC strain 1 as compared to the same cell strain transfected with human scrambled siRNA control under the same conditions (Fig. 5A). As expected, PGI2 production decreased substantially after human COX-1-10aa-PGIS knockdown (51±7.3% reduction compared to scrambled siRNA control, $P<0.05$, n=3; Fig. 5B). A similar siRNA approach was used to knockdown human COX-1, and PGI2 production was significantly reduced in PGI2-EPC strain 1 after human COX-1 siRNA transfection (64±2.9% reduction compared to scrambled siRNA control, $P<0.05$, n=3).

Accordingly, the total length of tubes formed in PGI2-EPCs transfected with PGIS siRNA was 33% ($P<0.05$; n=3) less than those in PGI2-EPCs transfected with control siRNA (Fig. 5C and 5D). The decreased paracrine effect on angiogenesis was detected in CM of PGI2-EPCs after COX-1-10aa-PGIS knockdown. CM, collected 96 hour after PGIS siRNA delivery into PGI2-EPCs, induced a total tube length that was 40% ($P<0.05$; n=3) shorter than those induced by CM from PGI2-EPCs after control siRNA delivery (Fig. 5E and 5F). Together, our findings indicate that PGI2-EPCs showed enhanced intrinsic angiogenesis ability and have the capacity to enhance tube formation in native EPCs through a paracrine mechanism.

PGI2-EPCs protect K^+ channel activity of vascular smooth muscle cells under hypoxia

As an endothelium-derived vasoactive mediator, PGI2 regulates vascular integrity and circulatory homeostasis (Duffy et al., 1999) and maintains vascular tone, in part, by relaxing underlying smooth muscle (Bellien et al., 2008; Feletou and Vanhoutte, 2006). Since PGI2-induced relaxation is largely attributed to SMC hyperpolarization through the activation of K^+ channels (Waldron and Cole, 1999), we examined whether enhanced release of PGI2 from PGI2-EPCs protects K^+ channel activity under harsh conditions such as hypoxia. Whole-cell patch-clamp experiments were performed to measure 4-aminopyridine–sensitive K^+ channel activity of rSMCs that had been cocultured with native EPCs or PGI2-EPCs under normal or hypoxic conditions. Under normoxic conditions, the K^+ channel activity of rSMCs was similar after being cocultured with either native EPCs or PGI2-EPCs; however, under hypoxic conditions, the K^+ channel activity of rSMCs was inhibited after being cocultured with native EPCs but was unaffected by hypoxia after coculture with PGI2-EPCs (Figs. 6A to 6C). The average current-voltage (I–V) data at endpoint amplitude showed that the 4-aminopyridine–sensitive K^+ current density was significantly increased in rSMCs cocultured under hypoxic conditions with PGI2-EPCs when compared to rSMCs similarly cocultured with native EPCs (7.50±1.59pA/pF vs. 3.99±1.26 pA/pF, respectively; $P<0.01$; n=9). In addition, we performed experiments using siRNA to downregulate COX-1-10aa-PGIS activity. After PGIS siRNA knockdown of COX-1-10aa-PGIS in PGI2-EPCs, coculture experiments failed to show enhanced K^+ current density of rSMCs (4.80±0.34 pA/pF; $P<0.05$; n=9), compared to cocultured PGI2-EPCs treated with control siRNA (9.25±0.53 pA/pF; Figs. 6D and 6E). Therefore, our data illustrate the protective effects of PGI2-EPCs on K^+ channel activity of SMCs under hypoxic conditions, which is crucial for the maintenance of vascular tone.

Discussion

In the present study, we have stably transduced rat outgrowth EPC strains with a novel active human triple-catalytic hybrid enzyme COX-1-10aa-PGIS (PGI2-EPCs). The engineered PGI2-EPCs constitutively secreted over 3 times more endogenous PGI2than native EPCs. Furthermore, we have shown that the PGI2-EPCs have enhanced intrinsic angiogenic potency and provide protection of function for both EPCs and SMCs. By establishing these PGI2-EPC strains, we have provided the groundwork for an innovative approach to PGI2 pharmacotherapy. The delivery of PGI2-EPCs into injured tissue may lead to repopulation of the damaged vasculature and restoration of vascular tone balance.

Prostacyclin is synthesized from AA in a multistep process involving the enzymes COX-1 and PGIS. In addition to the prostaglandins, the AA pathway synthesizes the vasoconstrictor TXA2. PGI2 counteracts TXA2-induced cardiovascular injury (eg, platelet aggression and atherosclerosis). Reduced PGI2 production in cardiovascular patients results in an imbalance between PGI2 and TXA2, thus facilitating disease progression. By constructing a novel fusion enzyme (COX-1-10aa-PGIS), we integrated the 3 required enzymatic activities for PGI2 production into a single protein to preferentially augument the production of PGI2 and

not TXA2. Increased PGI2 production could treat PGI2 deficiency by restoring normal levels of prostacyclin. The restoration of balance between PGI2 and TXA2 is critical for maintaining vascular homeostasis.

Our goal is to use cell therapy to treat cardiovascular diseases such as PAH. Intravenous therapy with prostacyclin is currently the only treatment for PAH that provides symptom improvement and a modest survival advantage, if administered long term (McLaughlin et al., 2009; McLaughlin et al., 2002). However, multiple disadvantages are associated with intravenous prostacyclin therapy. A few agents with longer half-lives (eg, iloprost and treprostinil) have been developed but require continuous intravenous or subcutaneous infusion, or numerous inhalation sessions. No effective oral prostacyclin analogues have been developed. A nonprostanoid prostacyclin-receptor agonist is under development, but the current data indicate it is not as effective as prostacyclin (Kuwano et al., 2007). Therefore, the introduction of a single-use or even periodically used cell-based therapy could significantly reduce costs and substantially improve quality of life for PAH patients.

Although the precise definition of EPCs has not been established, studies have demonstrated the regenerative potential of outgrowth EPCs derived from the bone marrow (Hirschi et al., 2008). These progenitor cells can home to damaged tissue and contribute to the growth and development of new blood vessels. Therefore, the strategy of using EPCs for therapeutic angiogenesis to achieve neovascularization holds promise. However, the function of EPCs may be affected by cardiovascular events and risk factors (Hill et al., 2003). Decreased numbers and reduced regenerative capacity of circulating EPCs are observed in the elderly and in populations at high risk for cardiovascular disease (Schmidt-Lucke et al., 2005; Vasa et al., 2001). Improving EPC function in patients may provide a new therapeutic approach to reduce future cardiovascular episodes.

PGI2 is important for the regenerative competence of EPCs (He et al., 2008). He and colleagues (He et al., 2008) noted that EPCs released higher amounts of PGI2 than did mature endothelial cells. This increased biosynthesis of PGI2, produced via the arachidonic pathway, is responsible for the enhanced proangiogenic properties of EPCs. Because EPC function depends on PGI2 production, the intrinsic neovascular-promoting properties of EPCs could be boosted by promoting the preferential production of PGI2. Thus, introducing the active hybrid enzyme (COX-1-10aa-PGIS) into EPCs isolated from high-risk cardiovascular patients may reverse the reduced function of EPCs in cardiovascular patients, in part, by augmenting PGI2 biosynthesis. Our data suggest that PGI2-EPCs not only showed enhanced intrinsic angiogenic properties as compared to native EPCs, but also extended their proangiogenic benefits by promoting tube formation in native EPCs via paracrine action. Transfection of PGI2-EPCs with PGIS siRNA knocked down the production of the COX-1-10aa-PGIS protein, attenuating the angiogenic properties of the transfected cells as illustrated by decreased incorporation of tubular structures and decreased paracrine effects on native EPCs. Given the short half-life of PGI2 and the difference between the extent of fusion protein reduction and the percentage decrease of total tube length as a result of human PGIS silencing (Fig. 4), supplementary angiogenic factors, other than PGI2, likely contributed to paracrine-mediated angiogenesis of PGI2-EPCs. This finding indicates the need for further proteomic analysis of CM to identify other paracrine modulators.

Endothelial dysfunction decreases endogenous PGI2 biosynthesis and induces contractility of underlying vascular SMCs (Vanhoutte, 2009). The triggered SMC activity stimulates multiple pathologic processes that ultimately result in damage to the blood vessels. To reverse the pathologic consequence induced by defective endothelial cells, the ideal therapeutic EPC should be able not only to incorporate into the local endothelium to

compensate for the loss of endothelial function but also to inhibit the activation of underlying SMCs by releasing endothelium-dependent hyperpolarizing factors, such as nitric oxide and/or PGI2, to induce smooth muscle relaxation (Bellien et al., 2008; Parkington et al., 2004). PGI2-EPCs are likely to achieve both of these benefits. In the present study, we found that the hyperpolarization of the SMC membrane (measured by increasing 4-AP-sentitive K^+ channel activity) under hypoxic conditions was significantly enhanced in SMCs cocultured with PGI2-EPCs compared with SMCs cocultured with native EPCs. Thus, our findings suggest that PGI2-EPCs can resist an adverse environment and provide better intrinsic endothelial function than native EPCs.

Conclusion

We have stably transduced rat outgrowth EPCs with a novel COX-1-10aa-PGIS plasmid that promotes intrinsic PGI2 biosynthesis. No viral vectors were used during nucleofection, thus eliminating the possibility of insertional mutagenesis. PGI2-EPC strains provided multiple benefits including improved angiogenesis and K^+-mediated SMC cell hyperpolarization under hypoxic conditions. Our findings suggest that using PGI2-EPCs may provide an innovative way to increase the efficiency of cell therapy in cardiovascular patients. Additional work is ongoing to examine the in vivo biologic activity of PGI2-EPCs.

Acknowledgments

Contract grant sponsor: National Heart, Lung and Blood Institute

Contract grant number: RC1HL100807

References

Asahara T, Masuda H, Takahashi T, Kalka C, Pastore C, Silver M, Kearne M, Magner M, Isner JM. Bone marrow origin of endothelial progenitor cells responsible for postnatal vasculogenesis in physiological and pathological neovascularization. Circ Res. 1999; 85:221–228. [PubMed: 10436164]

Asahara T, Murohara T, Sullivan A, Silver M, van der Zee R, Li T, Witzenbichler B, Schatteman G, Isner JM. Isolation of putative progenitor endothelial cells for angiogenesis. Science. 1997; 275:964–967. [PubMed: 9020076]

Badesch DB, McLaughlin VV, Delcroix M, Vizza CD, Olschewski H, Sitbon O, Barst RJ. Prostanoid therapy for pulmonary arterial hypertension. J Am Coll Cardiol. 2004; 43:56S–61S. [PubMed: 15194179]

Barst RJ, Rubin LJ, Long WA, McGoon MD, Rich S, Badesch DB, Groves BM, Tapson VF, Bourge RC, Brundage BH, et al. A comparison of continuous intravenous epoprostenol (prostacyclin) with conventional therapy for primary pulmonary hypertension. The Primary Pulmonary Hypertension Study Group. N Engl J Med. 1996; 334:296–302. [PubMed: 8532025]

Bellien J, Thuillez C, Joannides R. Contribution of endothelium-derived hyperpolarizing factors to the regulation of vascular tone in humans. Fundam Clin Pharmacol. 2008; 22:363–377. [PubMed: 18705747]

Duffy SJ, Castle SF, Harper RW, Meredith IT. Contribution of vasodilator prostanoids and nitric oxide to resting flow, metabolic vasodilation, and flow-mediated dilation in human coronary circulation. Circulation. 1999; 100:1951–1957. [PubMed: 10556220]

Feletou M, Vanhoutte PM. Endothelium-derived hyperpolarizing factor: where are we now? Arterioscler Thromb Vasc Biol. 2006; 26:1215–1225. [PubMed: 16543495]

He T, Lu T, d'Uscio LV, Lam CF, Lee HC, Katusic ZS. Angiogenic function of prostacyclin biosynthesis in human endothelial progenitor cells. Circ Res. 2008; 103:80–88. [PubMed: 18511850]

Hill JM, Zalos G, Halcox JP, Schenke WH, Waclawiw MA, Quyyumi AA, Finkel T. Circulating endothelial progenitor cells, vascular function, and cardiovascular risk. N Engl J Med. 2003; 348:593–600. [PubMed: 12584367]

Hirschi KK, Ingram DA, Yoder MC. Assessing identity, phenotype, and fate of endothelial progenitor cells. Arterioscler Thromb Vasc Biol. 2008; 28:1584–1595. [PubMed: 18669889]

Ingram DA, Mead LE, Tanaka H, Meade V, Fenoglio A, Mortell K, Pollok K, Ferkowicz MJ, Gilley D, Yoder MC. Identification of a novel hierarchy of endothelial progenitor cells using human peripheral and umbilical cord blood. Blood. 2004; 104:2752–2760. [PubMed: 15226175]

Kawabe J, Yuhki K, Okada M, Kanno T, Yamauchi A, Tashiro N, Sasaki T, Okumura S, Nakagawa N, Aburakawa Y, Takehara N, Fujino T, Hasebe N, Narumiya S, Ushikubi F. Prostaglandin I2 promotes recruitment of endothelial progenitor cells and limits vascular remodeling. Arterioscler Thromb Vasc Biol. 2010; 30:464–470. [PubMed: 20007911]

Kuwano K, Hashino A, Asaki T, Hamamoto T, Yamada T, Okubo K, Kuwabara K. 2-[4-[(5,6-diphenylpyrazin-2-yl)(isopropyl)amino]butoxy]-N-(methylsulfonyl)acetam ide (NS-304), an orally available and long-acting prostacyclin receptor agonist prodrug. J Pharmacol Exp Ther. 2007; 322:1181–1188. [PubMed: 17545310]

Liu Q, Chen ZQ, Bobustuc GC, McNatt JM, Segall H, Pan S, Willerson JT, Zoldhelyi P. Local gene transduction of cyclooxygenase-1 increases blood flow in injured atherosclerotic rabbit arteries. Circulation. 2005; 111:1833–1840. [PubMed: 15824211]

McLaughlin VV, Archer SL, Badesch DB, Barst RJ, Farber HW, Lindner JR, Mathier MA, McGoon MD, Park MH, Rosenson RS, Rubin LJ, Tapson VF, Varga J, Harrington RA, Anderson JL, Bates ER, Bridges CR, Eisenberg MJ, Ferrari VA, Grines CL, Hlatky MA, Jacobs AK, Kaul S, Lichtenberg RC, Moliterno DJ, Mukherjee D, Pohost GM, Schofield RS, Shubrooks SJ, Stein JH, Tracy CM, Weitz HH, Wesley DJ. Accf/Aha. ACCF/AHA 2009 expert consensus document on pulmonary hypertension: a report of the American College of Cardiology Foundation Task Force on Expert Consensus Documents and the American Heart Association: developed in collaboration with the American College of Chest Physicians, American Thoracic Society, Inc., and the Pulmonary Hypertension Association. Circulation. 2009; 119:2250–2294. [PubMed: 19332472]

McLaughlin VV, Shillington A, Rich S. Survival in primary pulmonary hypertension: the impact of epoprostenol therapy. Circulation. 2002; 106:1477–1482. [PubMed: 12234951]

Mitchell JA, Warner TD. COX isoforms in the cardiovascular system: understanding the activities of non-steroidal anti-inflammatory drugs. Nat Rev Drug Discov. 2006; 5:75–86. [PubMed: 16485347]

Moncada S, Gryglewski R, Bunting S, Vane JR. An enzyme isolated from arteries transforms prostaglandin endoperoxides to an unstable substance that inhibits platelet aggregation. Nature. 1976; 263:663–665. [PubMed: 802670]

Murata T, Ushikubi F, Matsuoka T, Hirata M, Yamasaki A, Sugimoto Y, Ichikawa A, Aze Y, Tanaka T, Yoshida N, Ueno A, Oh-ishi S, Narumiya S. Altered pain perception and inflammatory response in mice lacking prostacyclin receptor. Nature. 1997; 388:678–682. [PubMed: 9262402]

Numaguchi Y, Naruse K, Harada M, Osanai H, Mokuno S, Murase K, Matsui H, Toki Y, Ito T, Okumura K, Hayakawa T. Prostacyclin synthase gene transfer accelerates reendothelialization and inhibits neointimal formation in rat carotid arteries after balloon injury. Arterioscler Thromb Vasc Biol. 1999; 19:727–733. [PubMed: 10073980]

Parkington HC, Coleman HA, Tare M. Prostacyclin and endothelium-dependent hyperpolarization. Pharmacol Res. 2004; 49:509–514. [PubMed: 15026028]

Ruan KH, So SP, Cervantes V, Wu H, Wijaya C, Jentzen RR. An active triple-catalytic hybrid enzyme engineered by linking cyclo-oxygenase isoform-1 to prostacyclin synthase that can constantly biosynthesize prostacyclin, the vascular protector. FEBS J. 2008; 275:5820–5829. [PubMed: 19021758]

Schmidt-Lucke C, Rossig L, Fichtlscherer S, Vasa M, Britten M, Kamper U, Dimmeler S, Zeiher AM. Reduced number of circulating endothelial progenitor cells predicts future cardiovascular events: proof of concept for the clinical importance of endogenous vascular repair. Circulation. 2005; 111:2981–2987. [PubMed: 15927972]

Shi Q, Rafii S, Wu MH, Wijelath ES, Yu C, Ishida A, Fujita Y, Kothari S, Mohle R, Sauvage LR, Moore MA, Storb RF, Hammond WP. Evidence for circulating bone marrow-derived endothelial cells. Blood. 1998; 92:362–367. [PubMed: 9657732]

Takahashi T, Kalka C, Masuda H, Chen D, Silver M, Kearney M, Magner M, Isner JM, Asahara T. Ischemia- and cytokine-induced mobilization of bone marrow-derived endothelial progenitor cells for neovascularization. Nat Med. 1999; 5:434–438. [PubMed: 10202935]

Vanhoutte PM. Endothelial dysfunction: the first step toward coronary arteriosclerosis. Circ J. 2009; 73:595–601. [PubMed: 19225203]

Vasa M, Fichtlscherer S, Aicher A, Adler K, Urbich C, Martin H, Zeiher AM, Dimmeler S. Number and migratory activity of circulating endothelial progenitor cells inversely correlate with risk factors for coronary artery disease. Circ Res. 2001; 89:E1–7. [PubMed: 11440984]

Waldron GJ, Cole WC. Activation of vascular smooth muscle K+ channels by endothelium-derived relaxing factors. Clin Exp Pharmacol Physiol. 1999; 26:180–184. [PubMed: 10065344]

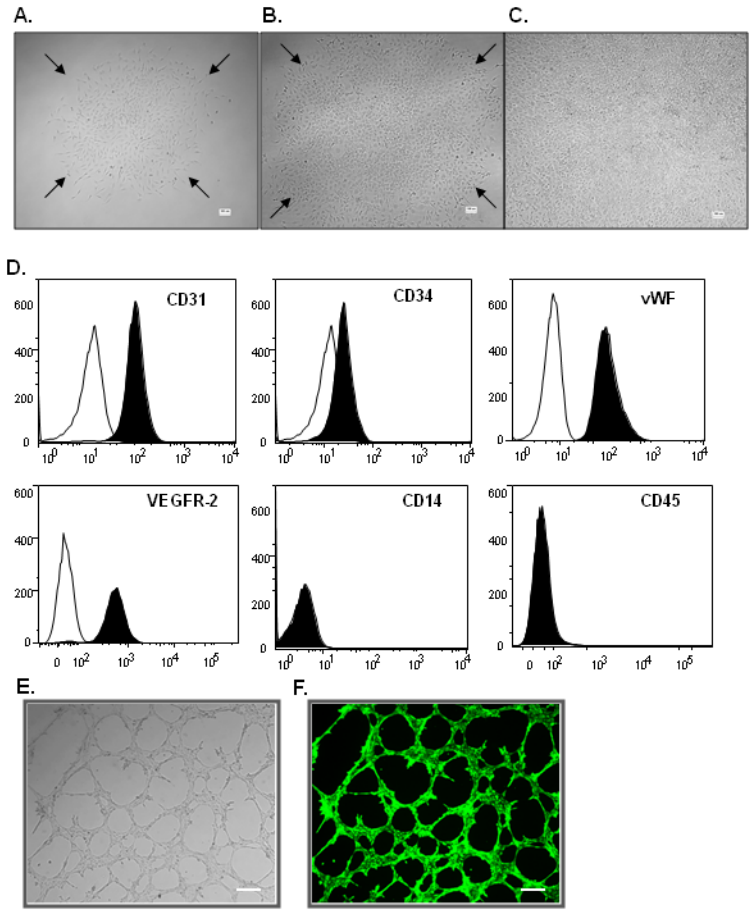

Figure 1.

Surface antigen profile and tube formation of outgrowth EPCs (native EPCs). **(A, B)** Representative light micrographs of outgrowing endothelial cell colonies derived from rat bone marrow mononuclear cells. (**C**) Confluent cell monolayer formed by outgrowth EPCs. Scale bar= 100μm. **(D)** Flow cytometry analysis showed that EPCs express CD31, CD34, vWF, and VEGFR-2, but not CD14 and CD45. (**E)** Representative light micrograph of tube-like structures formed by EPCs. Scale bar=50μm. (**F)** Representative fluorescent micrograph of tube-like structures stained with Calcein AM (viability dye). Scale bar= 50μm.

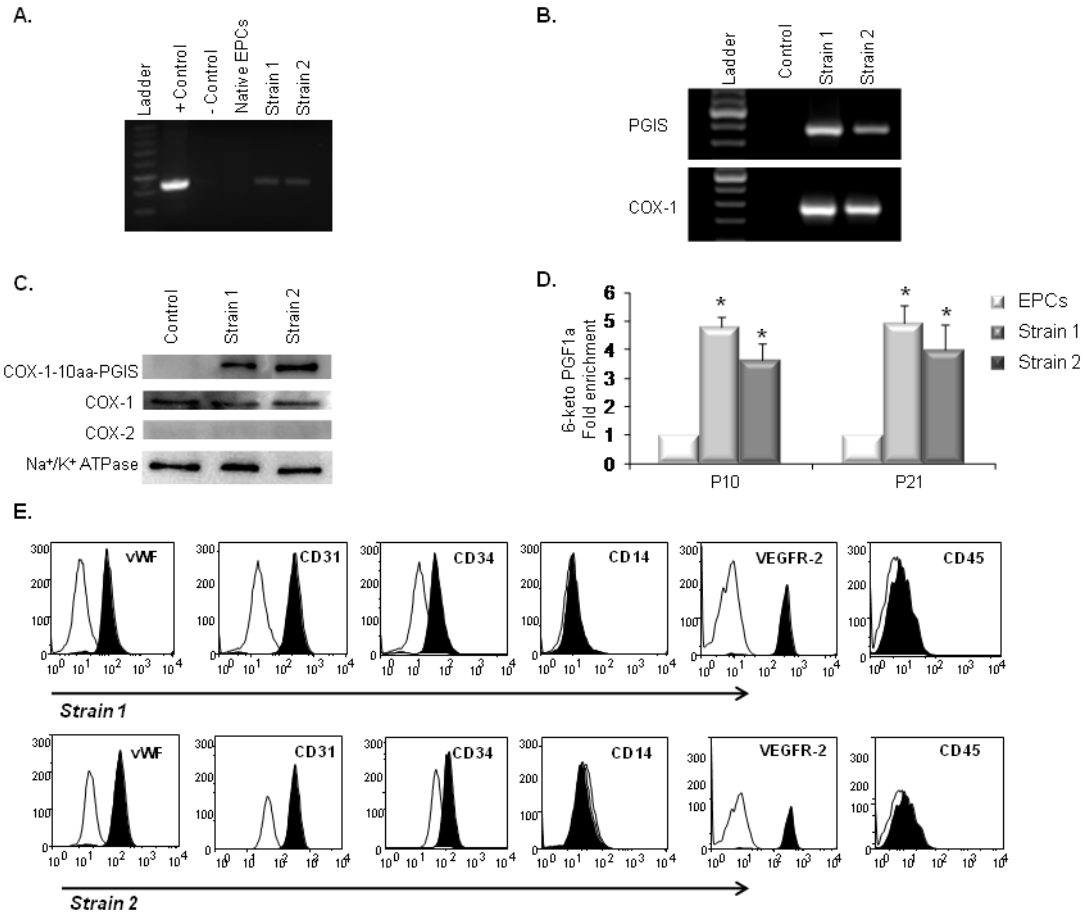

Figure 2.

Characterization of PGI2-EPC strains that overexpress active triple-catalytic enzyme. **(A)** PCR showed the integration of the COX-1-10aa-PGIS transgene into genomic DNA in strain 1 and 2 EPCs. The plasmid encoding COX-1-10aa-PGIS was used as the positive control; an empty vector served as the negative control. **(B)** RT-PCR detected human COX-1 and PGIS transcripts in rat EPC strains 1 and 2. **(C)** Western blots showed the overexpression of COX-1-10aa-PGIS fusion protein (130 kD) in strain 1 and 2 EPCs. PGI2-EPC strains expressed endogenous COX-1 at a similar level as native EPCs (control). No endogenous COX-2 expression was detected by Western blot. Na^+/K^+ ATPase protein served as a loading control. **(D)** PGI2-EPC strains consistently produced significantly higher levels of PGI2 than native EPCs. To assess prostacyclin production, the metabolite 6-keto PGF1α was measured by enzyme immunoassay in the supernatants after cells were grown under endothelial conditions for 24 hours (n=3). Native EPCs served as a control in **B–D**. **P*<0.05 compared to control. **(E)** Representative flow cytometry analysis showed that PGI2-EPC strains 1 and 2 retained similar expression levels of CD31, CD34, vWF, VEGFR-2, CD14, and CD45 as compared to those of native EPCs (displayed in Fig.1D), n=3.

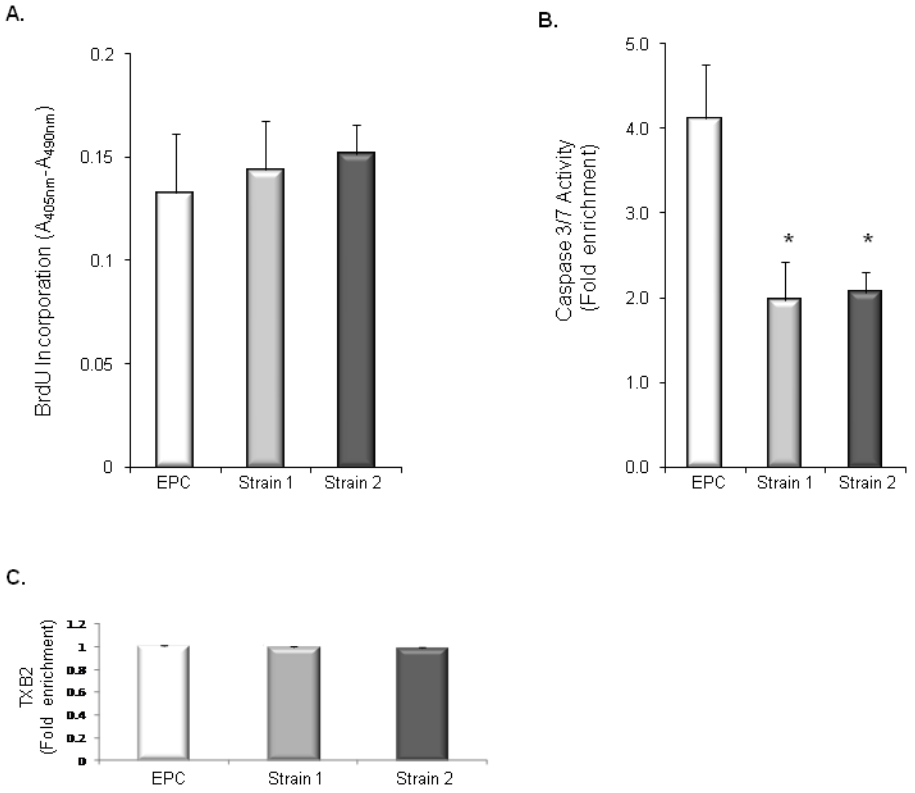

Figure 3. PGI2-EPC proliferation and apoptosis

(A) BrdU incorporated into replicating DNA during PGI2-EPC proliferation at a similar rate as that in native EPCs. EPCs vs strain 1, $P>0.05$, n=3; EPCs vs strain 2, $P>0.05$, n=3. **(B)** PGI2-EPCs showed significantly decreased caspase-3/7 activity than did native EPCs after induction of apoptosis by hydrogen peroxide. *$P<0.05$ vs native EPCs, n=3. **(C)** PGI2-EPC strains secreted a similar amount of TXA2 as compared to native EPCs. TXB2 enzyme immunoassay was used to assess TXA2 production. EPCs vs. strain 1 & 2, $P>0.05$, n=3.

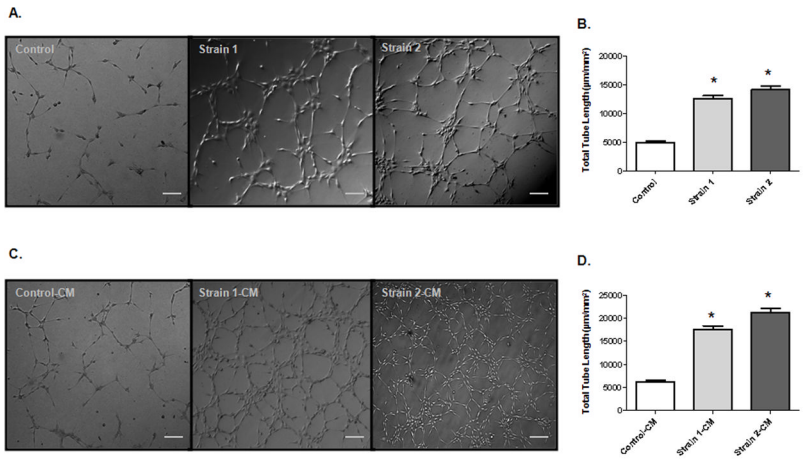

Figure 4.

PGI2-EPC strains promote in vitro angiogenesis. **(A)** Representative images of tubes formed in native EPCs (control) and PGI2-EPCs (strains 1 and 2) after being seeded on a reduced growth factor–membrane matrix. Scale bar=50 μm. **(B)** Quantification of tube formation. Total tube length was measured as μm/mm^2, n=3; **P*<0.05 vs control. **(C)** Representative images of tube formation in native EPCs in the presence of conditioned medium (CM) from native EPCs (control CM) and PGI2-EPCs (strain 1 and 2 CM). Scale bar=50 μm. **(D)** Quantification of tube formation. Total tube length was measured as μm/mm^2, n=3; **P*<0.05 vs control-CM.

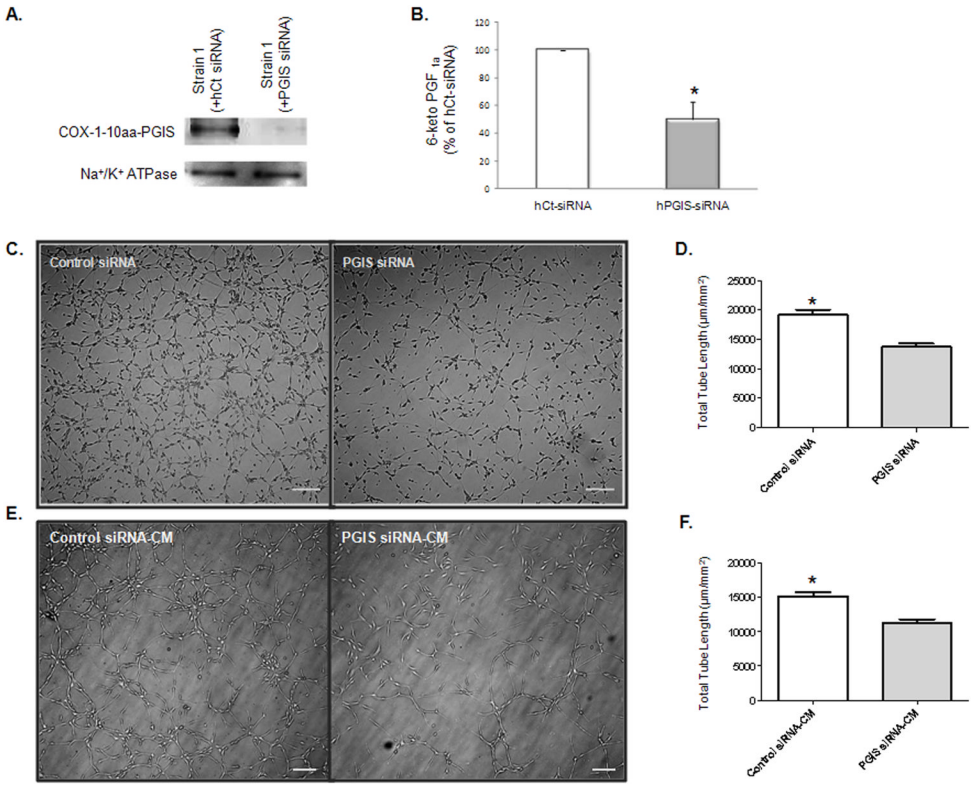

Figure 5.

Knockdown of hybrid enzyme expression in PGI2-EPCs decreased in vitro angiogenesis. **(A)** Western blot showed a significant reduction of COX-1-10aa-PGIS fusion protein in PGIS-EPC strain 1 after silencing of the human PGIS gene. Na^+/K^+ ATPase protein served as a loading control. **(B)** siRNA knockdown of human PGIS reduced prostacyclin production in the supernatant of PGI2-EPC strain 1. **P*<0.05 compared to PGIS siRNA; n=3. **(C)** Representative images of tubular structures. Scale bar=50 μm. **(D)** Quantification of tube formation. Tube formation assays were performed 96 hours after transfection of human PGIS siRNA or control siRNA transfection into PGI2-EPCs. Total tube length was measured as μm/mm^2, n=3; **P*<0.05 compared to PGIS siRNA. **(E)** Representative images of tubular structures of native EPCs in the presence of conditioned medium (CM), which was collected 96 hours after PGIS siRNA or control siRNA transfection, respectively. Scale bar=50 μm. **(F)** Quantification of tube formation. Total tube length was measured as μm/mm^2, n=3; **P*<0.05 compared to PGIS siRNA-CM.

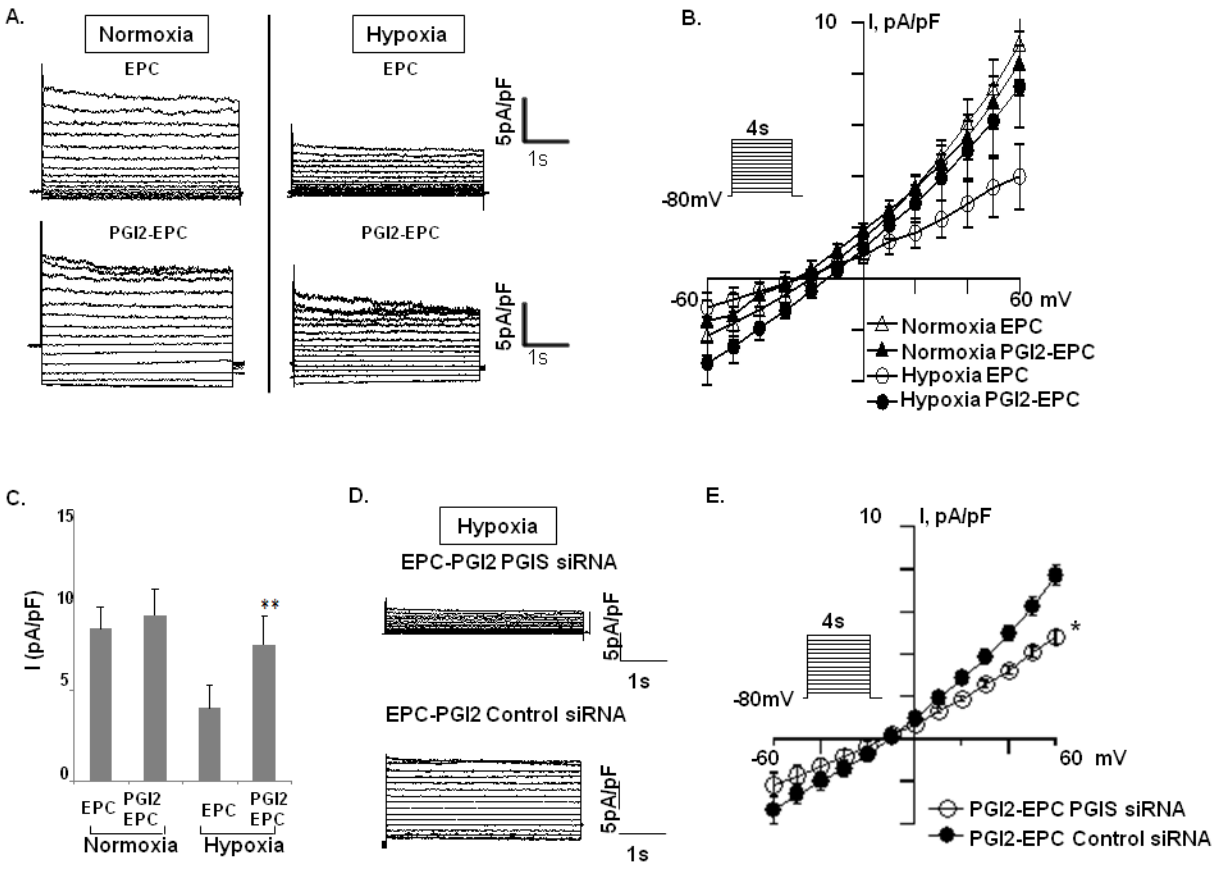

Figure 6.

Paracrine effects of native EPCs and PGI2-EPCs on 4-aminopyridine–sensitive K^+ current of rat smooth muscle cells (rSMCs) under normoxia and hypoxia. **(A)** Representative current traces were elicited by depolarizing voltage pulses (4 s) between −70 and +60 mV (10 mV steps) from a holding potential of −80mV under normoxic and hypoxic conditions. **(B)** Average data showing current-voltage (*I–V)* relationships. **(C)** Summarized data showing current amplitudes at 60 mV (n=9). ***P*<0.01 compared with rSMCs cocultured with native EPCs. **(D)** Representative current traces were recorded from rSMCs after coculture with PGI2-EPCs treated with PGIS siRNA or PGI2-EPCs treated with control siRNA under hypoxia. **(E)** The current-voltage (*I–V)* relationships (n=9). **P*<0.05 compared with rSMCs cocultured with PGI2-EPCs treated with PGIS siRNA.